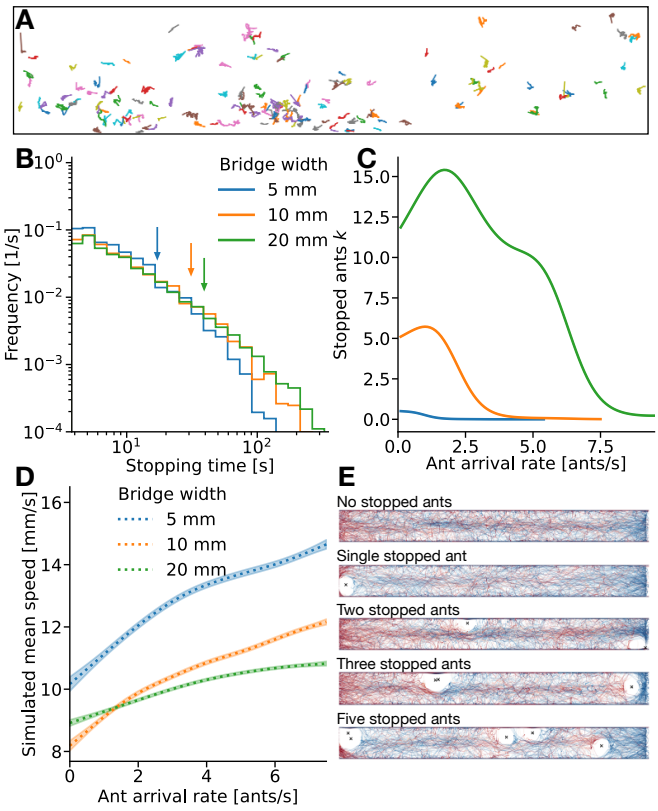

FIG. 3. **Ant speed depends on ant influx and stopped individuals.** (A) Positions of stopped ants over a 10-minute interval. (B) Histogram showing the time ants stop for. Arrows indicate the average stopping time. (B) Average number of ants stopped as a function of the ant arrival rate. (D) Average ant speed versus ant arrival rate from individual-based simulations when stopped ants are present (three, five, and ten stopped ants for the 5, 10, and 20 mm bridge, respectively). (C) Simulated ant tracks (red tracks start at the left end, while blue tracks start at the right end of the bridge) with 0, 1, 2, and 5 (top to bottom) obstacles inserted at random points on the bridge for a constant ant arrival rate of 5 ants/s.

ants (Fig. 3C). Crucially, the narrower the bridge, the smaller the number of stopped ants.

From this data, we hypothesized that stopped ants actively shape traffic into narrower channels by artificially reducing the available space. In our simulation model, we implemented different numbers of stopped ants at random positions on the bridge to understand how their traffic influences the transport across the bridge. Simulated ant trajectories avoided the stopped ants, creating space devoid of traffic (Fig. 3E). Indeed, stopped ants cause the simulated mean speed across the bridge to drop at low ant arrival rates. As a result, the model incorporating stopped ants captures the experimental data well (Fig. 3E).

E. Artificial obstacles play a similar role to stopped ants

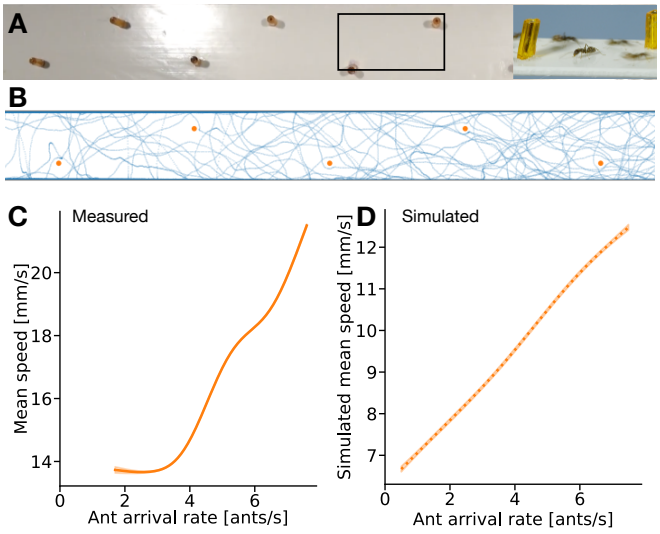

FIG. 4. **Artificial obstacles affect the traffic flow similarly to stopped individuals.** (A) Experimental setup of a bridge of 10 mm with pillars. (B) Simulation showing pillars in orange and ant tracks over 100 s in blue. (C) Average ant speed as a function of ant arrival rate (measured over 10 s time intervals) for bridges with artificial obstacles. (D) Simulated average ant speed as a function of ant arrival rate with artificial obstacles.

To test this further, we introduced artificial obstacles (pillars) in a regular pattern across the 10 mm bridge (Fig. 4A) connected to a colony of approximately 25 600 individuals. This caused ants at low arrival rates (up to 3 ants/s) to move substantially faster (13.5 mm/s, up to twice the speed) than in the same bridge without obstacles (compare Fig. 1D and Fig. 4C). At higher arrival rates, we observe a sharp increase in the mean speed up to 20 mm/s (Fig. 4C). In all, the pillars reduce the space available to ants, leading to an increased speed and shifting the curve in Fig. 1D so that the plateau is attained at lower ant arrival rates (we cannot access an analogous sharp increase beyond 14 mm/s in the case without obstacles, which might occur for ant arrival rates higher than 8 ants/s). In the presence of pillars, we found virtually no stopped ants in the bridge (Fig. S6). This supports our hypothesis that pillars can replace the role of stopped ants in actively shaping traffic by reducing the available space. To validate it, we implemented pillars in our model arranged in the same regular pattern as in the experiments (Fig. 4B). We find that the simulated mean speed describes the experimental data with pillars well (Fig. 4D). Comparing the results with pillars or stopped ants, we find that in experiments, the regular arrangement of pillars produces larger speeds than the corresponding experiment of dynamically stopped ants (Appendix, Fig. S8A). In the case of simulations, the same

is true only at high densities, with the effect reversed at lower densities (Appendix, Fig. S8B).

III. DISCUSSION

In this paper, we demonstrated that ants autonomously regulate their own traffic and effectively overcome environmental constraints. Our findings reveal a remarkable efficiency in ant transport, particularly under high-density conditions, where typical traffic systems, such as pedestrian or vehicular models, would predict a decline in speed. Contrary to these systems, we observed that not only does the flux (or transport rate) remain high at elevated densities, but the velocity of individual ants also reaches its maximum in high-traffic situations (Fig. 1). This result challenges conventional traffic dynamics, where increased density generally leads to slower movement, even if the overall flow is maintained.

We developed an agent-based model simulating ant movement along the bridge to interpret these observations further. This model allowed us to examine the underlying mechanisms driving this unique traffic behavior. Our analysis suggests that when traffic density is moderate, ants coordinate their movements by having a fraction of individuals stop. These stationary ants reduce the effective cross-sectional area of the bridge, thereby concentrating the movement into a narrower, more efficient region. This counterintuitive behavior–where stopped ants enhance overall flow–was supported by our simulations, which revealed that the presence of motionless ants is crucial for replicating the experimental results.

To validate our hypothesis, we introduced artificial obstacles in both experiments and simulations to mimic the effect of stopped ants. With these regularly spaced pillars in place, we observed fewer stationary ants, yet the traffic flow remained efficient. This suggests that the artificial obstacles replicate the function of the stopped ants by inducing a higher density in localized areas, thus reducing the need for ants to halt. Our findings confirm that these obstacles optimize traffic flow in a manner similar to the natural stoppage behavior of the ants.

These results offer a novel perspective on traffic regulation strategies in biological systems, where crowding can paradoxically lead to improved transport efficiency. In the case of Argentine ants, this improvement seems to arise from enhanced coordination and more directed movement under crowded conditions. This form of dynamic, self-organized traffic management, where individuals adjust their behavior to maximize collective efficiency, could have implications beyond ant colonies. Our findings suggest potential applications in human traffic systems, particularly in crowded environments such as stadiums or transit hubs. By strategically incorporating obstacles or barriers, achieving optimal flow while maintaining safety may be possible [27–30], offering new insights into the design of more efficient pedestrian traffic systems [31]. Studies on pedestrians indicate that the spatial layout of obstacles is important [32]. While our focus was on the effect of stopped individuals on the flow, we also observed that the spatial arrangement of such individuals can play a role.

METHODS

Experimental protocol

The experimental data used for the analyses in (sections without pillars) was taken from [22]. Here, we briefly summarise their experimental protocol; full details can be found in [22]. In the experiments, a colony of Argentine ants *Linepithema humile* was connected to a food source using a bridge of 170 mm in length. To manipulate density, the authors used a combination of bridges of different widths (5, 10, and 20mm) and experimental colonies of various sizes (from 400 to 25 600 ants) (see Fig. 1A, [22]). They conducted a total of 170 experiments. The size and design of the food source were such that it never saturated, even for the largest colony size.

In this paper, we introduced a new experiment conducted with the 10 mm and the 20 mm wide bridges similar to the one used by [22]. We glued eight pillars on the bridge, materialized by cylindrical plastic beads (4mm high, 1mm wide). The pillars were 2cm apart and placed in a staggered pattern (see Fig. 4). We run four replicates of this experiment following the same protocol as in [22]. Before each replicate, the experimental colonies were starved for five days, and the experiment started when the ants were given access to a food source placed on a platform (120x120 mm) at the other end of a plastic bridge. The total length of the bridge was 170mm. The food consisted of a 1M sucrose solution contained in 16 grooves (185mm long) carved in a block of plexiglas. The grooves were numerous enough to prevent crowding effects at the food source. The whole experimental set-up was isolated from any sources of disturbance by surrounding it with white paper walls.

Data collection, extraction, and analysis

Throughout the experiments, the traffic on the bridge was filmed from above for 60 minutes, starting as soon as the first ant entered the bridge. We used two cameras (Canon LEGRIA HF G30): one was filming the entire set-up, and the second one was focused on the bridge. We analyzed 116 videos among the 170 available, using trackR [33] to extract the trajectories of individual ants (see Fig. 1B). We tracked a central portion of the bridge with a length of 100 mm. In Figs. 2, 3, and 4, we only use the data once a steady bidirectional flux along the bridge has been attained.

To calculate the relationship between the mean ant speed and the ant arrival rate, we divided each exper-

iment into 10 s intervals and counted how many ants arrived at the bridge. For each interval, we averaged the individual speeds of all ants on the bridge throughout that interval. We then fitted a GAM to the resulting mean ant speed versus ant arrival rate data using the `mgcv` package [34] in R (version 4.4.1), using six knots, restricted maximum likelihood as the smoothing parameter estimation method, and a Gaussian distribution with the identity link function (Figs. 1D and 4C).

To identify stopped ants, we looked for parts of individual ant tracks that did not move more than 1 mm in any given 4 s interval. We gathered information on how long ants stay stopped according to these criteria (Fig. 3B). We also counted how many ants were stopped on average throughout each 10 s time window and again fitted a GAM to the resulting stopped ants vs ant arrival rate data, using 6 knots and a Poisson distribution with a logarithmic link function (Fig. 3C).

Agent-based model

Ants are modeled as interacting active Brownian particles, where the ith ant with center $\mathbf{X}_i(t) = (X_i(t), Y_i(t))$ and orientation $\Theta_i(t)$ at time t evolves according to

$$\mathrm{d}\mathbf{X}_i = v_0 \mathbf{e}(\Theta_i)\mathrm{d}t - \sum_{j\neq i} \nabla u(|\mathbf{X}_i - \mathbf{X}_j|)\mathrm{d}t, \tag{1a}$$

$$\mathrm{d}\Theta_i = \sqrt{2D}\mathrm{d}W_i. \tag{1b}$$

Here v_0 is the (fixed) self-propulsion speed, $\mathbf{e}(\theta) = (\cos\theta, \sin\theta)$ is the ant direction, D is the rotational diffusion coefficient, and W_i are independent one-dimensional Brownian motions. The ants interact through a repulsive exponential potential $u(r) = C_r \exp(-r/l_r)$, where C_r and l_r are the interaction's strength and range, respectively. Pheromone deposition and trails are not included in (1) since its effect is negligible given the experiment bridge geometry and level of crowding.

We simulate the tracked central portion of the bridge, that is, the domain $(x, y) \in [-50, 50] \times [-w/2, w/2]$. Ants are released at $x = \pm 50$ mm uniformly distributed in y and with orientations $\cos(\theta) = \pm 1$, respectively. The boundaries $x = \pm 50$ mm are absorbing (when an ant arrives there, it is removed from the simulation). In experiments, some ants can walk sideways along the bridge ends $y = \pm w/2$. In the simulations, we model it as a slip boundary: if an ant hits $y = \pm w/2$, we project its direction $\mathbf{e}(\Theta)$ along the bridge, becoming $\mathbf{e}(\Theta) = (\mathrm{sgn}(\cos(\Theta)), 0)$ (see Fig. 2D). In the simulations with pillars (Fig. 4D), the interaction between an ant and a pillar is modeled with the same interaction potential u as the ant-ant interaction. Trajectories of (1) are simulated with an Euler–Maruyama scheme with $\Delta t = 0.1$ s using `Agents.jl`. The parameter values, obtained by fitting to the experimental data, are $v_0 = 15.5$ mm/s, $D_R = 0.38$ rad^2/s, $C_r = 129$ mm^2/s and $l_r = 3.96$ mm (see Appendix for details).

In simulations with k stopped ants, we choose k random positions on the bridge at the start of the simulation run and placed ants held motionless at those positions throughout the simulation at these positions.

For each value of the ant arrival rate, we ran 200 realizations of 100 seconds each. We ascertained that the ant traffic reached a steady state after at most 50 s and used the latter 50 s of each realization to calculate the average speed of ants. We fitted the same GAM model to the simulated data as for the experiments, except for the number of knots (we used ten instead of 6 knots, Figs. 2E, 3D and 4D).

ACKNOWLEDGMENTS

UD acknowledges funding from the Isaac Newton Trust (G101121). SG was supported by the National Science Foundation under grant no #EF-2222418. MB acknowledges funding from the Royal Society (URF\R1\180040).

[1] I. Mellman and G. Warren, The road taken: past and future foundations of membrane traffic, Cell **100**, 99 (2000).
[2] G. van Niel, D. R. Carter, A. Clayton, D. W. Lambert, G. Raposo, and P. Vader, Challenges and directions in studying cell–cell communication by extracellular vesicles, Nature Reviews Molecular Cell Biology **23**, 369 (2022).
[3] J. Tu, K. Inthavong, and G. Ahmadi, *Computational fluid and particle dynamics in the human respiratory system* (Springer Science & Business Media, 2012).
[4] C. Seguin, M. P. Van Den Heuvel, and A. Zalesky, Navigation of brain networks, Proceedings of the National Academy of Sciences **115**, 6297 (2018).
[5] N. M. Coe and H. W.-C. Yeung, *Global production networks: Theorizing economic development in an interconnected world* (Oxford University Press, 2015).
[6] C. Bonansco and M. Fuenzalida, Plasticity of hippocampal excitatory-inhibitory balance: Missing the synaptic control in the epileptic brain, Neural Plasticity **2016**, 8607038 (2016).
[7] N. Shiwakoti, M. Sarvi, G. Rose, and M. Burd, Animal dynamics based approach for modeling pedestrian crowd egress under panic conditions, Procedia-social and behavioral sciences **17**, 438 (2011).
[8] D. Chowdhury, A. Schadschneider, and K. Nishinari, Physics of transport and traffic phenomena in biology: from molecular motors and cells to organisms, Physics of Life reviews **2**, 318 (2005).
[9] A. Dussutour, V. Fourcassié, D. Helbing, and J.-L. Deneubourg, Optimal traffic organization in ants under

crowded conditions, Nature **428**, 70 (2004).
[10] T. J. Czaczkes, C. Grüter, and F. L. Ratnieks, Negative feedback in ants: crowding results in less trail pheromone deposition, Journal of the Royal Society Interface **10**, 20121009 (2013).
[11] S. Wendt, N. Kleinhoelting, and T. J. Czaczkes, Negative feedback: ants choose unoccupied over occupied food sources and lay more pheromone to them, Journal of The Royal Society Interface **17**, 20190661 (2020).
[12] M. Moussaïd, D. Helbing, and G. Theraulaz, How simple rules determine pedestrian behavior and crowd disasters, Proceedings of the National Academy of Sciences **108**, 6884 (2011), 1105.2152.
[13] M. Moussaïd, S. Garnier, G. Theraulaz, and D. Helbing, Collective information processing and pattern formation in swarms, flocks, and crowds, Topics in Cognitive Science **1**, 469 (2009).
[14] D. Helbing, Traffic and related self-driven many-particle systems, Reviews of modern physics **73**, 1067 (2001).
[15] J. Duan, G. Zeng, N. Serok, D. Li, E. B. Lieberthal, H.-J. Huang, and S. Havlin, Spatiotemporal dynamics of traffic bottlenecks yields an early signal of heavy congestions, Nature communications **14**, 8002 (2023).
[16] M. Burd, D. Archer, N. Aranwela, and D. J. Stradling, Traffic dynamics of the leaf-cutting ant, atta cephalotes, The American Naturalist **159**, 283 (2002).
[17] I. D. Couzin and N. R. Franks, Self-organized lane formation and optimized traffic flow in army ants, Proceedings of the Royal Society of London. Series B: Biological Sciences **270**, 139 (2003).
[18] V. Fourcassié, A. Dussutour, and J.-L. Deneubourg, Ant traffic rules, Journal of Experimental Biology **213**, 2357 (2010).
[19] N. Gravish, G. Gold, A. Zangwill, M. A. Goodisman, and D. I. Goldman, Glass-like dynamics in confined and congested ant traffic, Soft matter **11**, 6552 (2015).
[20] C. Hönicke, P. Bliss, and R. F. Moritz, Effect of density on traffic and velocity on trunk trails of formica pratensis, The Science of Nature **102**, 1 (2015).
[21] D. Strömbom and A. Dussutour, Self-organized traffic via priority rules in leaf-cutting ants, PLoS Computational Biology **14**, e1006523 (2018).
[22] L.-A. Poissonnier, S. Motsch, J. Gautrais, J. Buhl, and A. Dussutour, Experimental investigation of ant traffic under crowded conditions, elife **8**, e48945 (2019).
[23] I. Prigogine, A boltzmann-like approach to the statistical theory of traffic flow, in *Theory of Traffic Flow*, edited by R. Herman (Elsevier, Amsterdam, 1961) p. 158.
[24] W. Luo, L. Sun, L. Yao, Q. Gong, and J. Rong, Experimental study for optimizing pedestrian flows at bottlenecks of subway stations, Promet-Traffic&Transportation **30**, 525 (2018).
[25] D. Helbing, I. J. Farkas, P. Molnar, and T. Vicsek, Simulation of pedestrian crowds in normal and evacuation situations, Pedestrian and evacuation dynamics **21**, 21 (2002).
[26] N. A. M. Araújo, L. M. C. Janssen, T. Barois, G. Boffetta, I. Cohen, A. Corbetta, O. Dauchot, M. Dijkstra, W. M. Durham, A. Dussutour, S. Garnier, H. Gelderblom, R. Golestanian, L. Isa, G. H. Koenderink, H. Löwen, R. Metzler, M. Polin, C. P. Royall, A. e. Šarić, A. Sengupta, C. Sykes, V. Trianni, I. Tuval, N. Vogel, J. M. Yeomans, I. Zuriguel, A. Marin, and G. Volpe, Steering self-organisation through confinement, Soft Matter **19**, 1695 (2023).
[27] G. A. Frank and C. O. Dorso, Room evacuation in the presence of an obstacle, Physica A: Statistical Mechanics and its Applications **390**, 2135 (2011).
[28] R. Yano, Effect of form of obstacle on speed of crowd evacuation, Physical Review E **97**, 032319 (2018).
[29] Y. Hu, Y. Bi, X. Ren, S. Huang, and W. Gao, Experimental study on the impact of a stationary pedestrian obstacle at the exit on evacuation, Physica A: Statistical Mechanics and its Applications **626**, 129062 (2023).
[30] Y. Zhao, T. Lu, L. Fu, P. Wu, and M. Li, Experimental verification of escape efficiency enhancement by the presence of obstacles, Safety science **122**, 104517 (2020).
[31] N. Shiwakoti and M. Sarvi, Enhancing the panic escape of crowd through architectural design, Transportation research part C: emerging technologies **37**, 260 (2013).
[32] S. Chen, L. Fu, J. Fang, and P. Yang, The effect of obstacle layouts on pedestrian flow in corridors: An experimental study, Physica A: Statistical Mechanics and its Applications **534**, 122333 (2019).
[33] S. Garnier, *trackR - Multi-object tracking with R* (2022), r package version 0.5.3.
[34] S. N. Wood, *mgcv: Mixed GAM Computation Vehicle with Automatic Smoothness Estimation* (2023), r package version 1.9-1.
[35] In fact, we also fitted the parameters using (5), and no noticeable difference to the resulting parameter values was found from the fitted values using (6).